Aus der Neurochirurgischen Klinik und Poliklinik

der Ludwig-Maximilians-Universität München

Direktor: Prof. Dr. med. Jörg-Christian Tonn

Decreased demand for olfactory periglomerular cells impacts on neural precursor cell viability in the rostral migratory stream

Dissertation

zum Erwerb des Doktorgrades der Medizin

an der Medizinischen Fakultät der

Ludwig-Maximilians-Universität zu München

vorgelegt von

Song Gu

aus Hefei, P.R. China

2018

Mit Genehmigung der Medizinischen Fakultät

der Universität München

Berichterstatter:

Prof. Dr. rer. nat. Rainer Glaß

Mitberichterstatter:

Prof. Dr. Jürgen Bernhagen

Prof. Dr. Olivier Gires

Prof. Dr. Armin Giese

Dekan:

Prof. Dr. med. dent. Reinhard Hickel

Tag der mündlichen Prüfung:

29.11.2018

Eidesstattliche Versicherung

Song, Gu
Name, Vorname

Ich erkläre hiermit an Eides statt,

dass ich die vorliegende Dissertation mit dem Thema

Decreased demand for olfactory periglomerular cells impacts on neural precursor cell viability in the rostral migratory stream

selbständig verfasst, mich außer der angegebenen keiner weiteren Hilfsmittel bedient und alle Erkenntnisse, die aus dem Schrifttum ganz oder annähernd übernommen sind, als solche kenntlich gemacht und nach ihrer Herkunft unter Bezeichnung der Fundstelle einzeln nachgewiesen habe.

Ich erkläre des Weiteren, dass die hier vorgelegte Dissertation nicht in gleicher oder in ähnlicher Form bei einer anderen Stelle zur Erlangung eines akademischen Grades eingereicht wurde.

Muich, 20.12.2018
Ort, Datum

Song Gu
Unterschrift Doktorandin/Doktorand

I. Contents

II. List of Figures

III. List of Tables

IV. Abbreviations

NPC	Neural Precursor Cell
SVZ	Sub-ventricular Zone
RMS	Rostral Migratory Stream
OB	Olfactory Bulb
OSC	Olfactory Sensory Cilia
OE	Olfactory Epithelium
CP	Cribriform Plate
OSN	Olfactory Sensory Neurons
GFAP	Glial Fibrillary Acidic Protein
BrdU	Bromodeoxyuridine
Mash1	Mammalian Achaete-scute Homologue 1
PSA-NCAM	Polysialylated Neural Cell Adhesion Molecule
Dcx	Doublecortin
Tuj1	Neuronal Class III β-tubulin
GDNF	Glial Cell Line-derived Neurotrophic Factor
ECM	Extra Cellular Matrix
MT1-MMP	Membrane-type 1 Matrix Metalloproteinases
OMP	Olfactory Marker Protein
TAM	Tumor-associated Myeloid Cells
TH	Tyrosine-hydroxylase
IPL	Internal Plexiform Layer

EPL	External Plexiform Layer
GL	Glomeruli Layer
RR	Respiration-entrained Rhythm
PLC	Prelimbic Cortex
PAC	Parietal Cortex

1. Introduction

1.1 Role of Neural Precursor Cells (NPCs)

Central nervous system diseases, like brain tumors, brain injuries or neurodegenerative diseases, often cause neuronal damage which can lead to poor prognosis and high incidence of disability in patients (Crane et al., 2016; Weller et al., 2015). There are currently no effective therapeutic strategies for addressing neurological deficits, since common treatments without repair of damaged neurons are normally not able to relieve all symptoms. Neurogenesis occurs in two stem cell niches of the adult brain, the dentate gyrus in the hippocampus and the sub-ventricular zone (SVZ), which is located along the lateral ventricles (Kriegstein & Alvarez-buylla, 2011). The neural precursor cells (NPCs) found in the hippocampus are well studied and have been discovered to have primary significance for learning, memory and various behaviors (Goncalves, Schafer, & Gage, 2016). The NPCs in the SVZ, on the other hand, have only been brought into focus in neuroscience research more recently, but it is now increasingly accepted that SVZ-derived adult neural stem cells have the ability to proliferate, migrate and differentiate and thus replace damaged neurons (Arvidsson, Collin, Kirik, Kokaia, & Lindvall, 2002).

In physiology, SVZ-derived NPCs mainly migrate through a pathway called the rostral migratory stream (RMS) toward the olfactory bulb (OB),

where they differentiate into olfactory interneurons (Belvindrah, Lazarini, & Lledo, 2009; Lazarini & Lledo, 2011). A fraction of NPCs also migrate through the medial migratory stream toward the prefrontal cortex (Sanai et al., 2012) and radially toward the frontal lobe (C. Ng et al., 2017), which might be related to evolutionarily-acquired brain functions. In the event of a brain injury, NPCs from the SVZ are redirected to lesion sites by several diffusible attractive factors, secreted by activated astrocytes, microglia, and vascular endothelial cells. At the site of injury, the NPCs then differentiate into functional neurons. All these indicate the significant therapeutic potential of NPCs (Arvidsson et al., 2002).

Despite this potential, however, the SVZ is not a viable therapeutic target for clinical medicine at present. This is largely because NPCs occur in high number in the central nervous systems of infants, but at much lower number in the brains of adults or the aged (Galvan & Jin, 2007; Klempin & Kempermann, 2007). Therefore SVZ-derived NPCs are not frequently enough to replace all the damaged neurons in a brain after a severe neuropathological incident. Unlike the situation that occurs along the SVZ-RMS-OB axis, also, there is no guiding structure leading the NPCs to the damaged brain area. Hence, NPC migration is less efficient and less target-directed in pathology (Zhang et al., 2007). In addition, only a fraction of recruited NPCs survive and differentiate into mature neurons

(Arvidsson et al., 2002). To find ways for increasing the number of NPCs which can migrate efficiently towards a damaged brain area, it is thus necessary to study the mechanisms controlling NPC proliferation and migration. While cell-division and migration regulating mechanisms in the embryonic and developing brain are relatively well studied, the mechanisms controlling cell proliferation and migration in the adult brain still need further exploration. In this aspect one particularly important question to be investigated is how (or whether) the division and migration of SVZ-derived NPCs is affected by external stimuli. One adequate external stimulus for NPCs in the SVZ-RMS-OB axis is olfaction. Hence, the primary goal for this study was to establish an experimental model to modulate olfactory sensory input to the OB and then observe NPC proliferation and migration under conditions of normal (control) or reduced olfactory sensory input.

1.2 NPC Subtypes and Migration Pathways

The SVZ-RMS-OB axis in rodents is an excellent system to investigate adult neurogenesis as well as NPC migration, differentiation and survival. The olfactory system of rodents is highly developed, consisting of olfactory sensory cilia (OSC), the olfactory epithelium (OE), cribriform plate (CP), OB, RMS and SVZ (DeMaria & Ngai, 2010). Olfactory sensory neurons (OSNs), which reside in the main olfactory epithelium,

can transmit olfactory signals from the nose to the OB (DeMaria & Ngai, 2010). The number of OSNs and connecting sensory neurons (between the OE and OB) is thus limited by the size of the olfactory epithelium. The activation of receptors within OSNs marks the beginning of the perception of odors. In response to an odor stimulus, the glomeruli in the OB recruit new interneurons generated from sub-ventricular NPCs throughout the whole lifetime (M. A. Hack et al., 2005). In particular, the SVZ contains neural stem cells (type-B cells), transit amplifying cells (type-C cells) and lineage-committed cells (type-A cells) (Kriegstein & Alvarez-buylla, 2011). Type-B cells are long-lived neural stem cells and infrequently enter the cell cycle. They can be immunohistochemically characterized by the co-expression of glial fibrillary acidic protein (GFAP) and nestin (Doetsch, García-Verdugo, & Alvarez-Buylla, 1997). Type-B cells can also be identified after systemic application of thymidine analogs bromodeoxyuridine (BrdU) which is incorporated into DNA during the cell cycle. Since type-B cells rarely enter an S-phase, they uptake BrdU only after prolonged application (repetitive application over three days or more) and BrdU will be retained for longer time periods (weeks and months) (Ramírez-Castillejo et al., 2006). Type-C cells, originating from type-B cells, are transient, fast proliferating, non-lineage committed cells and are immunopositive for mammalian achaete-scute homologue 1 (Mash1) (Lledo, Alonso, & Grubb, 2006). Type-C cells

quickly incorporate BrdU and can be labeled by a single, 2h BrdU-pulse. Type-C cells are the immediate precursors of type-A cells, which immunolabel for the markers nestin, polysialylated neural cell adhesion molecule (PSA-NCAM), doublecortin (Dcx) and neuronal class III β-tubulin (Tuj1) (Lledo et al., 2006). Type-A cells born in the SVZ migrate constitutively through the RMS into the OB where they detach from the pathway, integrate into granule and glomerular layers and differentiate into interneurons (Alvarez-Buylla & Lim, 2004). This direct, rapid and long-distance migration of NPCs is guided by directional cues provided along the migration pathway. Sonic hedgehog, one of the morphogens expressed in the SVZ, can attract type-A cells and regulate the number of neuroblasts migrating into the RMS (Angot et al., 2008). The type-A cells are then maintained in a tube-like structure formed of astrocytes. Hepatocyte growth factor, distributed throughout the RMS, attracts neuroblasts, and stimulates them to migrate within the pathway (Wang, Zhang, Gyetko, & Parent, 2011). Diffusible proteins such as Prokineticin-2, Netrin1, and glial cell line-derived neurotrophic factor (GDNF) produced by the OB can guide the NPCs towards their destination in the OB (Murase & Horwitz, 2002; K. L. Ng et al., 2005; Paratcha, Ibáñez, & Ledda, 2006). After reaching the OB, type-A cells radially migrate out from the RMS toward the granule cell layer and several extra cellular matrix (ECM) proteins such as Reelin, Tenascin-R,

and Prokineticin-2 control the detachment of NPCs from the RMS (I. Hack, Bancila, Loulier, Carroll, & Cremer, 2002; Lledo et al., 2006; K. L. Ng et al., 2005). Most neuroblasts differentiate into GABAergic neurons in granule layers while other sub-ventricular type-A cells migrate into the glomerular layer and become GABAergic periglomerular neurons (Lledo et al., 2006).

1.3 MT1-MMP Deficient Mouse Model

In the nasal cavity, nasal turbinate is made up of cartilage and forms the structural base of the OE. The development of nasal turbinate makes the inner face of nasal cavity curling and enlarges the inner surface of nasal cavity. The OE overlay on the surface of nasal turbinate, thus the area of the OE is closely related to the development of nasal turbinate (Gkantidis, Blumer, Katsaros, Graf, & Chiquet, 2012). OSNs reside within the OE, and the number of OSNs is thus directly correlated with the size of the OE. Therefore, the number of OSNs is indirectly dependent on the development of the nasal turbinate. In order to investigate whether significant changes occurs in the SVZ-RMS-OB axis in response to altered olfactory stimuli, both positive and negative modulation of olfactory inputs has been explored in different ways in previous studies. On the one side, studies have been performed to modify neurogenesis in the SVZ by enriching environmental factors (odorant enrichment), and it

was found that SVZ proliferation was only increased transiently in this case (Alonso et al., 2008). On the other side, olfactory sensory deprivation has been performed using different methods, such as bulbectomy or chemical induced lesions. However, inconsistent or even controversial results have been obtained. The controversial results of these studies are generally caused by different levels of cell-death or inflammation, and it is clear that pathological side-effects alone can modify SVZ plasticity and proliferation (Kazanis, 2009).

Building on this existing body of knowledge, our study sought to exploit a transgenic mouse model capable of overcoming these drawbacks. Membrane-type 1 matrix metalloproteinases (MT1-MMP) is closely related to turnover of type-II collagen, which impacts on cartilage formation (Holmbeck et al., 1999). In order to investigate the olfactory sensory innervation, olfactory marker protein (OMP) was used to detect OSNs (olfactory sensory neurons) in our previous studies (Langenfurth et al., 2016). OMP is a cytoplasmic signal transduction protein expressed in mature olfactory sensory neurons and an established marker for OSNs which connect the OE with the olfactory neuronal network within the OB (Oboti, Peretto, de Marchis, & Fasolo, 2011). In situ hybridization in the OMP was used to study the anatomy of the nasal turbinate and the overlaying olfactory epithelium in MT1-MMP deficient and MT1-MMP^{wt}

animals. The folding of nasal turbinate was reduced in MT1-MMP deficient mice resulting in decreasing olfactory epithelium surface as compared to the controls. In addition, in order to investigate if MT1-MMP also impacts on bone and cartilage structures and allows neuronal trajectories to project into the brain, we traced distinct OSNs from the nasal cavity into the olfactory bulb using mOR256-17-GFP mice crossbred with MT1-MMP deficient and MT1-MMP^{wt} animals. The mOR256-17-GFP mouse is an established transgenic mouse model in which cells expressing the odorant receptor mOR256-17 co-express the fluorescent marker tau-GFP (Luxenhofer, Breer, & Strotmann, 2008). In our results, the mOR256-17-GFP OSNs traversed the cribriform plate and entered the glomeruli correctly, while the number of olfactory sensory neurons was strongly reduced in MT1-MMP deficient mice compared to the controls (Langenfurth et al., 2016). Cranial development of MT1-MMP deficient mice was significantly affected, resulting in reduced folding in the nasal turbinate, in turn leading to reduced OSNs within the reduced superficial area of the OE. In situ hybridizations for the OMP (mature sensory neurons marker) and GAP43 (immature sensory neurons marker) showed that the correct anatomical layering for immature and mature sensory neurons was maintained in both MT1-MMP deficient mice and in the controls (Langenfurth et al., 2016). In situ hybridizations for the odorant receptors M72, mOR256-17 and mOR37A, revealed the

correct localization of these receptors within the olfactory epithelium (Langenfurth et al., 2016). Importantly, brain structures and cortical layers developed normally in both MT1-MMP deficient mice and controls (Langenfurth et al., 2016). Therefore, MT1-MMP deficiency did not affect olfactory epithelium and olfactory sensory neuron development. In addition, our previous study already showed that the numbers of microglia marker Iba1 positive cells did not increase in MT1-MMP deficient mice. Thus, these MT1-MMP deficient mice contained reduced numbers of newly-generated periglomerular neurons without any developmental deficits or pathological side effects such as inflammatory reactions in the brain. Within this study, the mouse model was further modified with bone-specific MT1-MMP ablation, with the key aim being to overcome the shortcomings of previous experimental approaches as discussed above.

1.4 Aim of the Study

It is a hallmark of adult neurogenesis to respond to physiological and pathological stimuli and to provide the cellular plasticity for learning, memory and brain repair. However, it is not known if constant physiological stimulation, e.g. through olfaction, is needed to maintain a basal level of sub-ventricular neurogenesis. In this study we thus aimed to investigate if a reduction in olfactory sensory innervation and OB size,

which implies a reduced demand for SVZ-derived type-A cells, results in altered neurogenesis in the SVZ. To explore this, a new transgenic mouse model was generated to allow study of the impact of modulated olfactory input under physiological conditions. More specifically, this model was used to investigate the role of the olfactory sensory system in controlling NPC proliferation, migration, differentiation and cell death in the SVZ. Furthermore, this model was used to analyze how altered sensory innervation changes the subtypes of newly-generated OB interneurons. Finally, It was used to explore whether putative stem cells in the RMS play a physiological role in animals with reduced OB-size.

Therefore, this study is mainly investigating the following questions:

1. To compare the level of fast proliferation (the overall number of type-C and type-A cells) and cell mortality in the SVZ of Osx-cre/MT1-MMP$^{-/-}$ mice versus Osx-cre/MT1-MMP$^{FL/WT}$ or Mt1-MMP$^{FL/FL}$ controls (are there differences within SVZ sub-regions?).

2. To compare the level of slow proliferation (the overall number of type-B cells) in the SVZ of Osx-cre/MT1-MMP$^{-/-}$ mice versus Osx-cre/MT1-MMP$^{FL/WT}$ or Mt1-MMP$^{FL/FL}$ controls (are there differences within SVZ sub-regions?).

3. To compare the level of proliferation, migration or cell death in the RMS of Osx-cre/MT1-MMP$^{-/-}$ mice versus Osx-cre/MT1-MMP$^{FL/WT}$ or Mt1-MMP$^{FL/FL}$ controls (are there differences within RMS sub-regions?).

2. Materials and Methods

2.1 Materials

2.1.1 Technical Equipment

Table 2.1.1 Technical Equipment

Lab Appliance	Company
Centrifuge	Thermo Fisher Scientific GmbH
Cryostat	Microtome, PFM AG
12 and 24-well Plates	TPP Techno GmbH
Incubator	Kendro GmbH
Laboratory Labeling System	LABXPERT TM
Microscope (fluorescence)-Axiovert 25	Carl Zeiss Microscopy GmbH
Microscope (transmitted light)-Axioskop 2	Carl Zeiss Microscopy GmbH
Microscope (confocal) TCS SP5	Leica Microsystems Vertrieb GmbH
Microscope Camera-AxioCam MRm	ZEISS GmbH
Microtome Slide 2003	PFM medical AG

2.1.2 Consumables

Table 2.1.2 Consumables

Product	Supplier
Tubes (0.5ml,1ml,2ml)	Eppendorf GmbH
Tubes (15ml,50ml)	VWR GmbH
Pipette tips (10µl, 20µl, 200µl ,1000 µl)	Eppendorf GmbH
Slides	Gerhard Menzel GmbH

Cover Slips	Gerhard Menzel GmbH
Tissue-Tek Cryomold (15mm×15mm×15mm)	Sakura Finetek USA
BrdU	Sigma GmbH
DAPI	Sigma GmbH
DAB and DAB-substrate	DCS Labline
Donkey Serum	Sigma GmbH
Dual Endogenous Enzyme Block	Dako
Ethanol-70%	CLN GmbH Chemikalien Laborbedarf
Ethanol-96%	CLN GmbH Chemikalien Laborbedarf
Ethanol-100%	CLN GmbH Chemikalien Laborbedarf
Eosin G-solution	Sigma GmbH
Ethylene	Sigma GmbH
Cryomatrix	Thermo Sientific
Glycerol	Sigma GmbH
Goat Serum	Sigma GmbH
Hematoxylin	Carl Roth GmbH
Ketamine	Zoetis Deutschland GmbH
0.9%Nacl	B.Braun Melsungen AG
Mounting Medium	IBIDI GmbH
Paraformaldehyde (PFA)	Sigma GmbH
Protein Block	Dako GmbH
Sucrose	Sigma GmbH
PBS	Apotheke Klinikum der Universität München
Triton X-100	Roche Diagnostics GmbH
Tween-20	Sigma GmbH
Xylol	Sigma GmbH

2.1.3 Antibodies

Table 2.1.3 (A) Primary Antibodies

Immunogen	Host Species	Isotype	Catalog number	Dilution	Provider
BrdU	Rat	IgG	OBT0030	1:500	AbD Serotec
Iba1	Rabbit	IgG	019-19741	1:500	Wako GmbH
CD68	Rat	IgG	MAC1957	1:200	AbD Serotec
CD209	Goat	lgG	IMG-6806A	1:200	Novus Biologicals
F4/80	Rat	IgG	Sc52664	1:200	Santa Cruz
Tyrosine-hydroxylase (TH)	Rabbit	IgG	Ab152	1:500	Millipore
Calbindin	Mouse	IgG	C9848	1:500	Sigma
Calretinin	Rabbit	IgG	610908	1:500	BD Bioscience
Nestin	Mouse	IgG	MAB353	1:200	Millipore
GFAP	Rabbit	IgG	Z0334	1:200	Dako
Mash1	Rabbit	IgG	Ab38556	1:500	Abcam
PSA-NCAM	Mouse	IgG	MAB5324	1:500	Millipore
Dcx	Mouse	IgG	sc-271390	1:100	Santa Cruz

Table 2.1.3 (B) Secondary Antibodies

Antigen	Host Species	Conjugation	Catalog number	Dilution	Provider
Rabbit IgG	Donkey	Alexa Fluor 488	711545152	1:500	Jackson Immuno-Research
Rabbit IgG	Donkey	Alexa Fluor 594	711585152	1:500	Jackson Immuno-Research
Rabbit IgG	Donkey	Cy3	71116152	1:500	Jackson Immuno-Research
Rabbit IgG	Donkey	biotinylated	711065152	1:250	Jackson Immuno-Research
Goat IgG	Donkey	Alexa Fluor 488	705545147	1:500	Jackson Immuno-Research
Rat IgG	Donkey	biotinylated	712065153	1:250	Jackson Immuno-Research
Rat IgG	Donkey	Alexa Fluor 488	712546153	1:250	Jackson Immuno-Research
Rat IgG	Donkey	Cy 3	712165150	1:250	Jackson Immuno-Research
Rat IgG	Donkey	Cy 5	712175150	1:250	Jackson Immuno-Research
Mouse IgG	Donkey	Alexa Fluor 488	715545150	1:500	Jackson Immuno-Research

2.1.4 Software

Table 2.1.4 Software

Software	Provider
Microsoft Office 2010	Microsoft
GraphPad Prism 6	Graph Pad Software
Image J	National Institutes of Health, USA
Adobe Photoshop CS 6	Adobe Systems

2.1.5 Animal Model

In this study, Osterix (Osx)-Cre mice were crossed with MT1-MMP$^{FL/FL}$ mice. Osx-cre/MT1-MMP$^{FL/FL}$ mice expressing cre-recombinase under control of the osteoblast-specific promoter element recombine (ablate) loxP-flanked sites of the MT1-MMP gene (Xu et al., 2016), which can thus lead to depletion of MT1-MMP, specifically within mesenchymal cells. As controls, there were 2 mouse groups: Osx-cre/MT1-MMP$^{FL/WT}$ and Mt1-MMP$^{FL/FL}$. At least 4 animals were included for each group.

For tracing the proliferation of NPCs, the thymidine analogue BrdU (5-bromo-2-deoxyuridine, at a concentration of 10mg/ml BrdU in sterile 0.9% NaCl solution) was injected at an effective concentration of 50mg/kg body weight 2h before euthanasia. Also, Mice were injected with 50 mg/kg BrdU i.p. 2x daily for three days to detect label-retaining cells (rarely proliferating type-B cells). Mice were then left untreated for

18 days; subsequently the animals were euthanized and prepared for immunolabeling studies.

2.2 Methods

2.2.1 Floating Section Preparation

Brains for immunohistochemical and histological studies were immersed in 4% PFA for 48 hours at +4°C, followed by incubation in 30% sucrose for 48 hours at +4°C. Samples were placed in Tissue-Tec, embedded with Cryo-Matrix and then stored in a -20℃ fridge. The frozen samples were then placed on a cryostat and cut horizontally or sagittally into 40μm sections. The sections were then collected systematically in 24-well plates filled with cryo-protectant (25% ethylene glycol and 25% glycerol in 0.1M PBS).

2.2.2 Immunohistochemistry

Samples were first incubated in 0.3% H_2O_2 in PBS for 15 min, followed by incubation with 5% donkey serum diluted in PBS for 1h for blocking. Primary antibodies diluted in 5% donkey serum were then applied to the samples. The samples stayed incubating in primary antibody at 4℃ in a cool room overnight. The secondary antibodies diluted in 5% donkey serum were applied to samples the next day and the samples were incubated with the secondary antibody for 2h at room temperature. Then

the samples were incubated with streptavidin-HRP for 1h in order to develop visible signals. The DAB solution was prepared to the suggested concentration and samples were left in DAB to develop signals for 3 min. In the end, the samples were mounted on slides and covered with cover slips.

2.2.3 Immunohistochemical Staining for BrdU

Bromodeoxyuridine (5-bromo-2-deoxyuridine, BrdU) is a synthetic analog of the nucleoside thymidine. It is incorporated into replicating DNA in dividing cells and can subsequently be detected by anti-BrdU antibodies (Wojtowicz & Kee, 2006). Frozen tissue sections were first fixed in 50% methanol, then incubated in HCl (2M) for 2h at room temperature to break the DNA structure of the BrdU-labeled cells. This was followed by an immediate neutralization through incubating the samples in borate buffer (0.1 M) for 5 min at room temperature. The standard staining procedure was then conducted as described previously. Between different solutions, samples were washed in PBS (pH 7.4), 3x, 5 min per wash. Finally, samples were left in DAB to develop signals and were mounted on slides.

2.2.4 H-E Staining

Sections were first mounted on slides. After the sections had dried on the

slides, they were immersed in 100% ethanol for 30s. Then the nuclei were stained with haematoxylin for 15 min. Then the samples were rinsed in running tap water for 5 min and immersed in eosin for 30s. Next the samples were dehydrated in sequence with 100%, 96%, 70% ethanol for 2 min, 2x each. Finally, the samples were immersed in xylol and then covered with cover slips.

2.2.5 Immunofluorescent Staining

Samples were first washed with PBT (PBS containing 0.1% Tween-20). Primary antibodies diluted in 5% donkey serum were then applied to the samples. The samples stayed incubating in primary antibody at 4℃ in a cool room overnight. The secondary antibodies diluted in 5% donkey serum were applied to samples the next day and the samples were then incubated with secondary antibody conjugated with fluorophore for 2h at room temperature. Finally, the samples were mounted on slides and covered with cover slips.

2.2.6 Regions of Interest (ROI) Definition

On the horizontal mouse brain slide, the ventricle shape varies in different layers of the brain, and the cell number between different layers is therefore non-comparable. 4 stereotactic coordinates (-2.04mm, -2.68mm, -3.16mm and -3.60mm to bregma) were defined as the ROIs and cell

number counting was performed separately for each animal. The coordinates were selected according to <The Mouse Brain in Stereotaxic Coordinates>. In the OB, the cell counting was also performed separately on slides of different coordinates. The ROIs were defined according to the different layers of OB structure, which were Internal Plexiform Layer (IPL), External Plexiform Layer (EPL) and Glomeruli layer (GL). The sagittal slides were mainly used for investigating the SVZ. Only the slides which revealed the entire RMS were selected for cell counting. The RMS was then divided into 3 parts according to location, the RMS1 (proximal to the SVZ), RMS2 and RMS3 (distal from the SVZ).

2.2.7 Evaluation of Staining

Immunohistochemical slides were evaluated at 20x magnification under the microscope. The total cell numbers, the BrdU(+) cell numbers, the Calbindin(+) cell numbers, Calretinin(+) cell numbers and Tyrosine hydroxylase(+) cell numbers were counted manually. Calbindin, Calretinin and Tyrosine hydroxylase were immune markers of main periglomerular interneuron subtypes. For each animal, the counting regions were counted 3 times, and the 20x scope for evaluation was chosen at random.

Immunoflourescent slides were evaluated with confocal microscopy. The

BrdU(+)Nestin(+)GFAP(+), BrdU(+)Mash1(+), BrdU(+)PAS-NCAM(+) cell numbers were counted manually for different NPC subtypes. BrdU(+)Nestin(+)GFAP(+) represent for Type-B cells, BrdU(+)Mash1(+) represent for Type-C cells and BrdU(+)PAS-NCAM(+) represent for Type-A cells. BrdU(+)Dcx(+) cell numbers were counted manually for migrating NPCs. Iba1(+)CD68(+), Iba1(+)CD209(+), Iba1(+)F4/80(+) cell numbers were counted manually for activated microglia and macrophages. For each animal, the counting regions were chosen at random and counted 3 times.

2.2.8 Statistical Analysis

Data sets were analyzed statistically using Prism 6 software and tested for normality via the Kolmogorov–Smirnov test. Two-sided levels of significance were determined at the $p < 0.05$ levels. Parametric testing was done via t-test. Significances are depicted as *: $p < 0.05$. Data are presented as mean ± SEM.

3. Results

3.1 Conditional MT1-MMP Deficiency Does Not Cause Inflammation in the Brain

Our previous study already showed that the number of microglia marker Iba1 positive cells did not increase in the brains of MT1-MMP deficient mice (Langenfurth et al., 2016). The experiment was repeated on conditional MT1-MMP deficient mice, combining another microglia immune-marker CD68 with Iba1 for identification of activated microglia (Glass & Synowitz, 2014). Iba1 was also combined with the markers indicating the functional states of myeloid cells (CD209 and F4/80) to detect activated microglia or macrophages (Glass & Synowitz, 2014; Graeber & Streit, 2010). With confocal imaging, we detected and confirmed the double positive cells. Again, the number of Iba1 positive microglia (also CD68 positive) remained unchanged in the conditional MT1-MMP deficient group. Expression levels for activation status markers in both conditional MT1-MMP deficient and control mice were very weak (F4/80) or even absent (CD209). For testing the validity of the immunolabeling paradigms, glioma samples were used, which contain large numbers of tumor-associated myeloid-cells (TAMs) and strongly express the immune markers mentioned above. These results support the view that conditional MT1-MMP deficient mice have no inflammatory reactions in the brain.

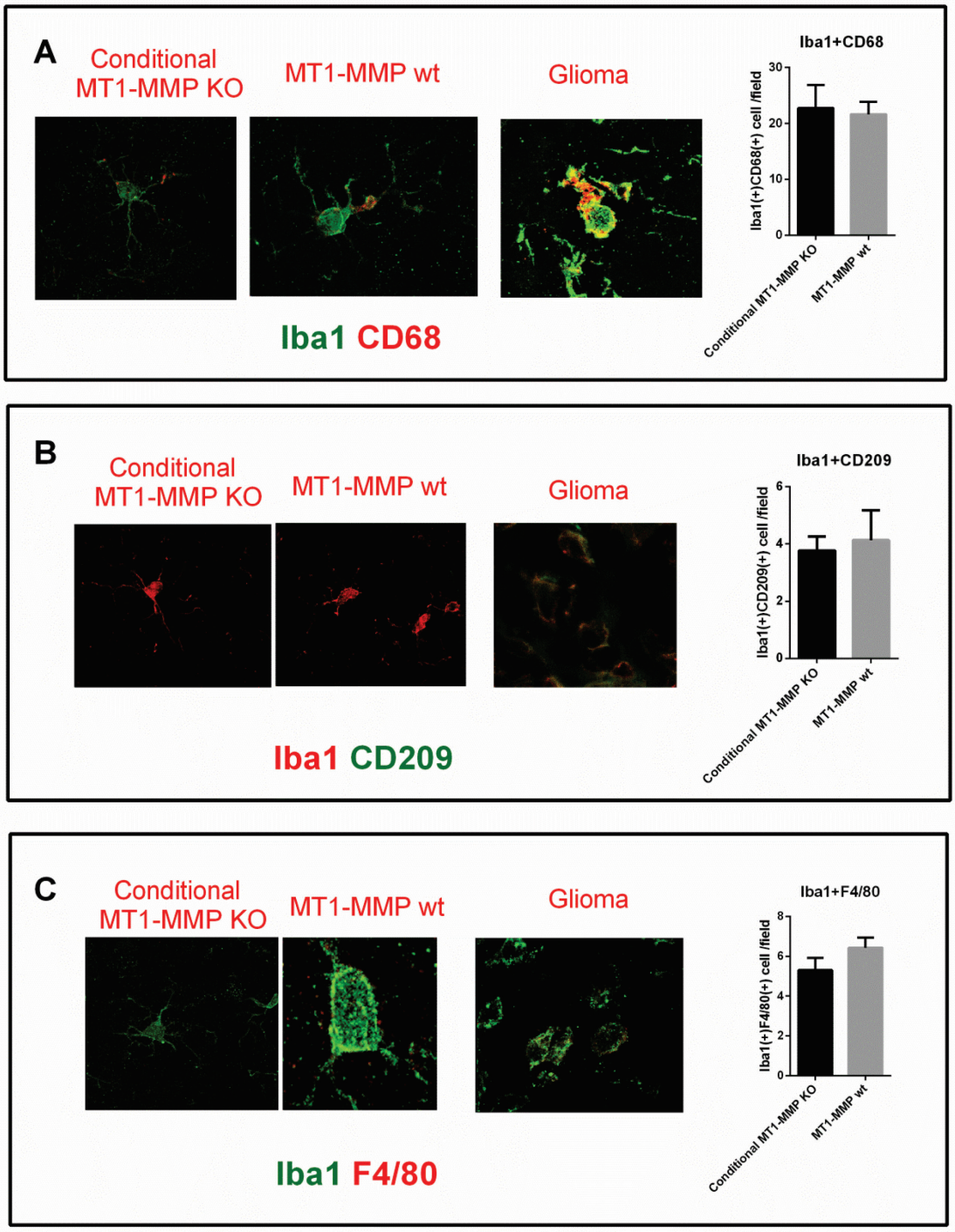

Figure 3.1 Immunoflourescent Staining for Immune Markers and Statistical Analysis.

This figure shows immunoflourescent double staining for immune markers in conditional MT1-MMP deficient mice, MT1-MMP^{wt} mice and mouse-harboring glioma. The bar chart shows the comparison of double positive cell numbers between conditional MT1-MMP deficient mice, MT1-MMP^{wt} mice and there is no significant difference in immune cell number between conditional MT1-MMP deficient mice and

MT1-MMP^{wt} mice. Iba1 and CD68, p=0.59 (A). Iba1 and CD209, p=0.61 (B). Iba1 and F4/80, p=0.06 (C).

3.2 Conditional MT1-MMP Deficiency Generates Reduced Demand of Periglomerular Interneurons.

3.2.1 Changes in OSNs and Size of OB

The previous findings already describe how germline and conditional MT1-MMP deficiency results in reduced sensory innervation of the OB. Statistically significant reduction in OB size was also observed in both germline and conditional MT1-MMP deficient mice as compared to controls. (Langenfurth et al., 2016)

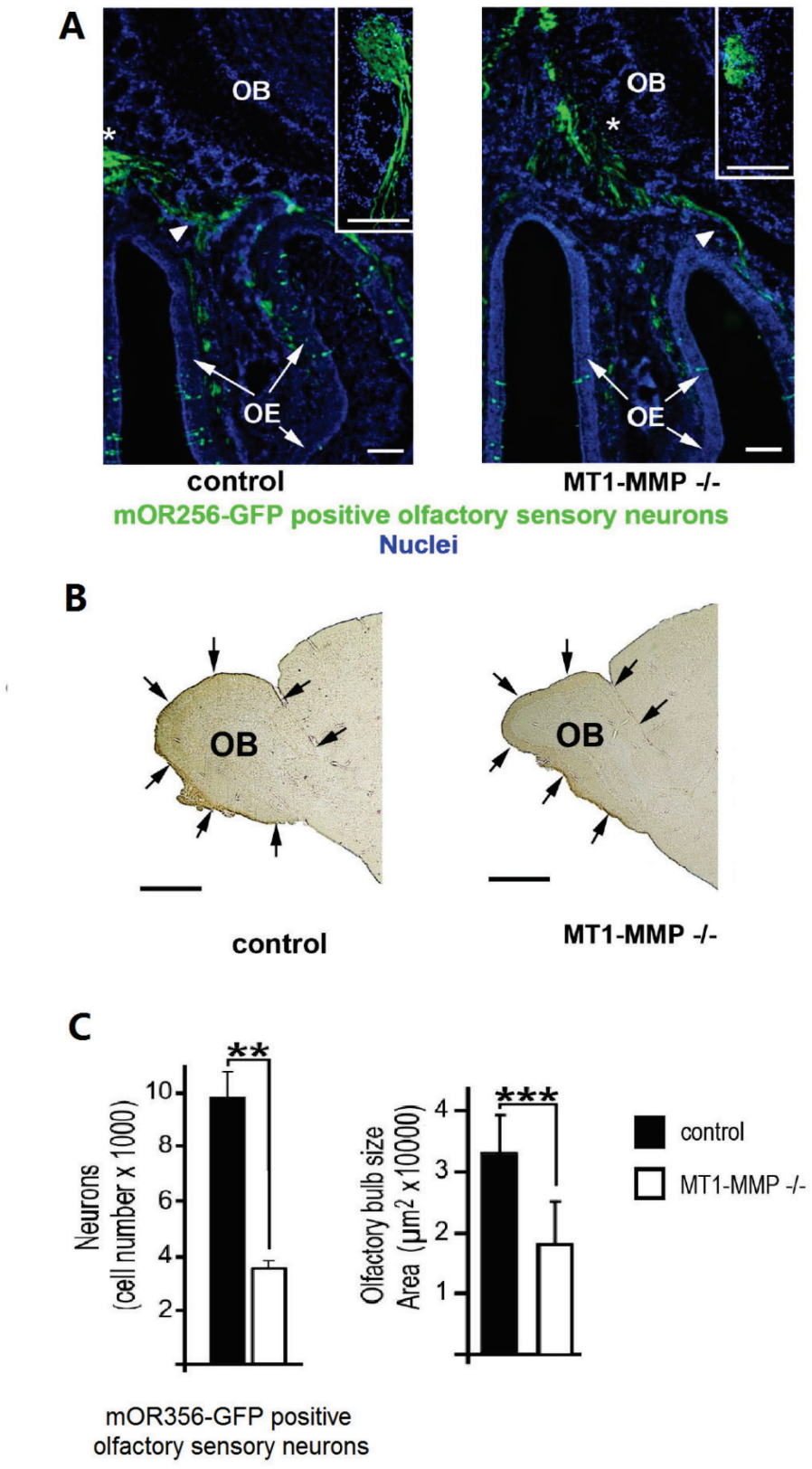

Figure 3.2.1 Comparison of The Number of mOR256-17-GFP Positive Neurons and The Size of OB

Fluorescent detection of OSNs in mOR256-17 reporter mice (mOR256-17-GFP crossed with MT1-MMP$^{-/-}$ or controls). OSNs expressing GFP is shown in green and nuclei are labeled with DAPI in blue. (A). Phase contrast images of a sagittal section through the OB in MT1-MMP$^{-/-}$ and controls (B). Bar chats shows the statistical analysis. The number of mOR256-17-GFP^{+} neurons was reduced in MT1-MMP$^{-/-}$ mice, $p < 0.005$; Olfactory bulb size is largely reduced in MT1-MMP$^{-/-}$ at P20, $p < 0.001$ (C).

3.2.2 Glomerulus in OB

Glomeruli, a spherical structure, are the basic subunits of glomerular layer. The olfactory nerve traverses the cribriform and form synapses to the interneurons in the glomeruli. To uncover what structure is affected within OB in the event of reduced OB size, H-E staining was performed on Osx-cre/MT1-MMP$^{FL/FL}$ and control mice. Slides with complete OB were selected to allow clear identification of the structure of the glomeruli. The number of glomeruli was counted for each animal and a significant reduction was observed in the Osx-cre/MT1-MMP$^{FL/FL}$ mice as compared to the two control groups. Furthermore, the cell numbers within individual glomeruli were counted to detect whether there was any change inside the glomerulus. However, there was no significant change between Osx-cre/MT1-MMP$^{FL/FL}$ and the two control groups. Finally, the diameter of the glomerulus was estimated and it was found that the average size of olfactory glomeruli was smaller in Osx-cre/MT1-MMP$^{FL/FL}$ mice compared to the controls.

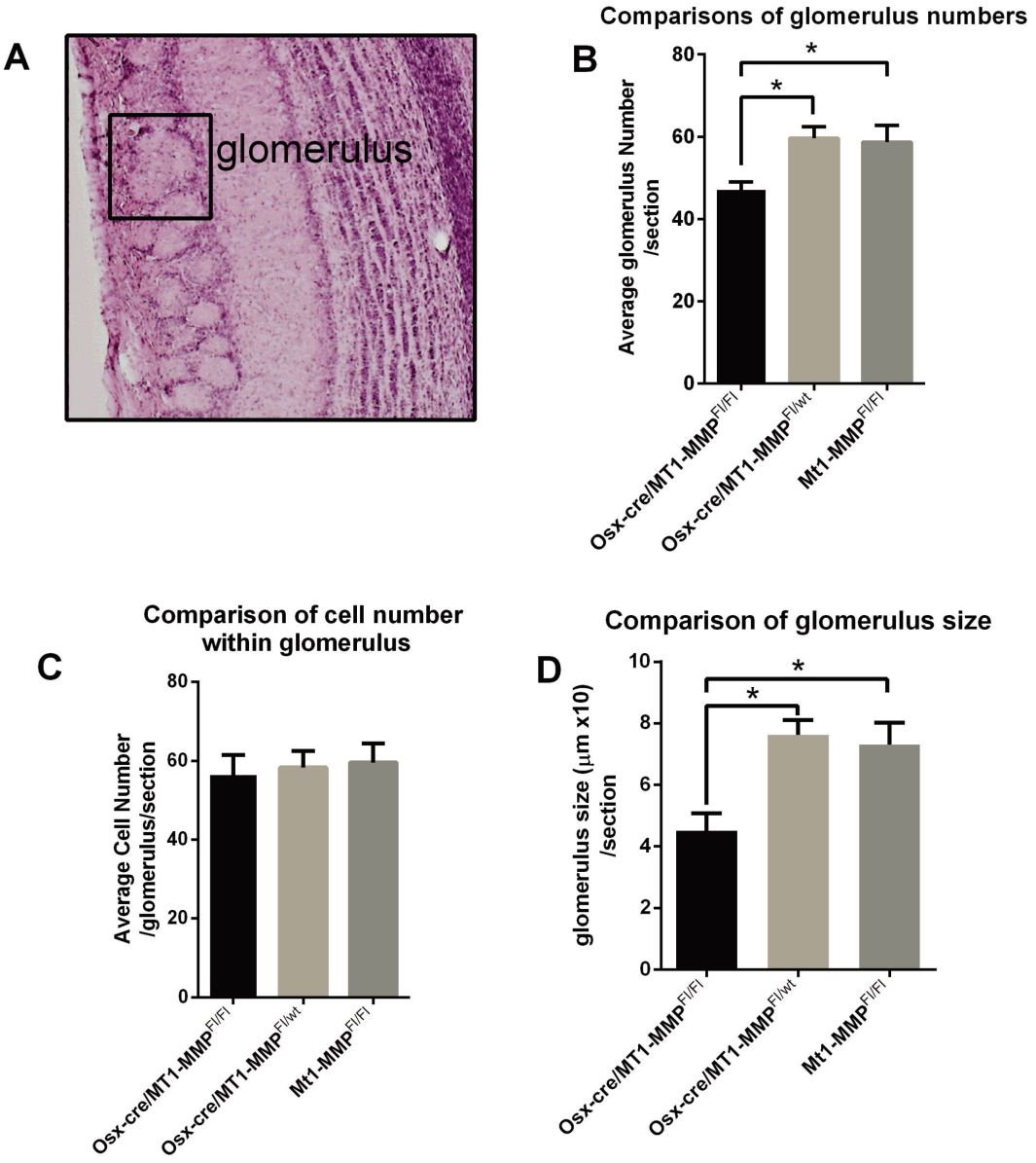

Figure 3.2.2 Comparison of Glomerulus Number, Average Cell Number Per Glomerulus and Glomerulus Size

H-E staining for OB (A). The glomerulus number was significantly reduced in the osx-cre/MT1-MMP$^{FL/FL}$ mice compared to either the Osx-cre/MT1-MMP$^{FL/wt}$ or the MT1-MMP$^{FL/FL}$ group, $p<0.0001$ and $p=0.0003$ (B). The average number per glomerulus was not significantly changed, $p=0.19$ and $p=0.06$ (C). The glomerulus size was significantly reduced in the Osx-cre/MT1-MMP$^{FL/FL}$ mice compared to either the Osx-cre/MT1-MMP$^{FL/wt}$ or MT1-MMP$^{FL/FL}$ group, $p < 0.005$ and $p < 0.005$ (D).

3.2.3 Interneurons in OB

As previously detailed, the glomeruli in the OB contain the terminals for the olfactory nerves as well as the interneurons and synapses between them. This study thus sought to explore how the interneurons within the OB changed in the pathological condition of reduced OB. To explore this, immunohistochemical staining was performed for the main subtypes of periglomerular neurons expressing tyrosine-hydroxylase (TH), calbindin or calretinin on Osx-cre/MT1-MMP$^{FL/FL}$ and control mice. The total cell number of each subtype of interneuron within the whole OB was then counted by sections. The number of interneurons significantly reduced in Osx-cre/MT1-MMP$^{FL/FL}$ mice as compared to control groups. The cell numbers of each interneuron subtype within glomeruli was then quantified. As with the total cell number, the number of interneurons per glomerulus remained unchanged. These results indicate that the reduced number of interneurons in the OB is not caused by any developmental deficits of the olfactory sensory system but rather by the reduced olfactory inputs (from the reduced OE surface area). This reduction in interneuron cell numbers generates a reduced demand for new neurons differentiating from migrating NPCs.

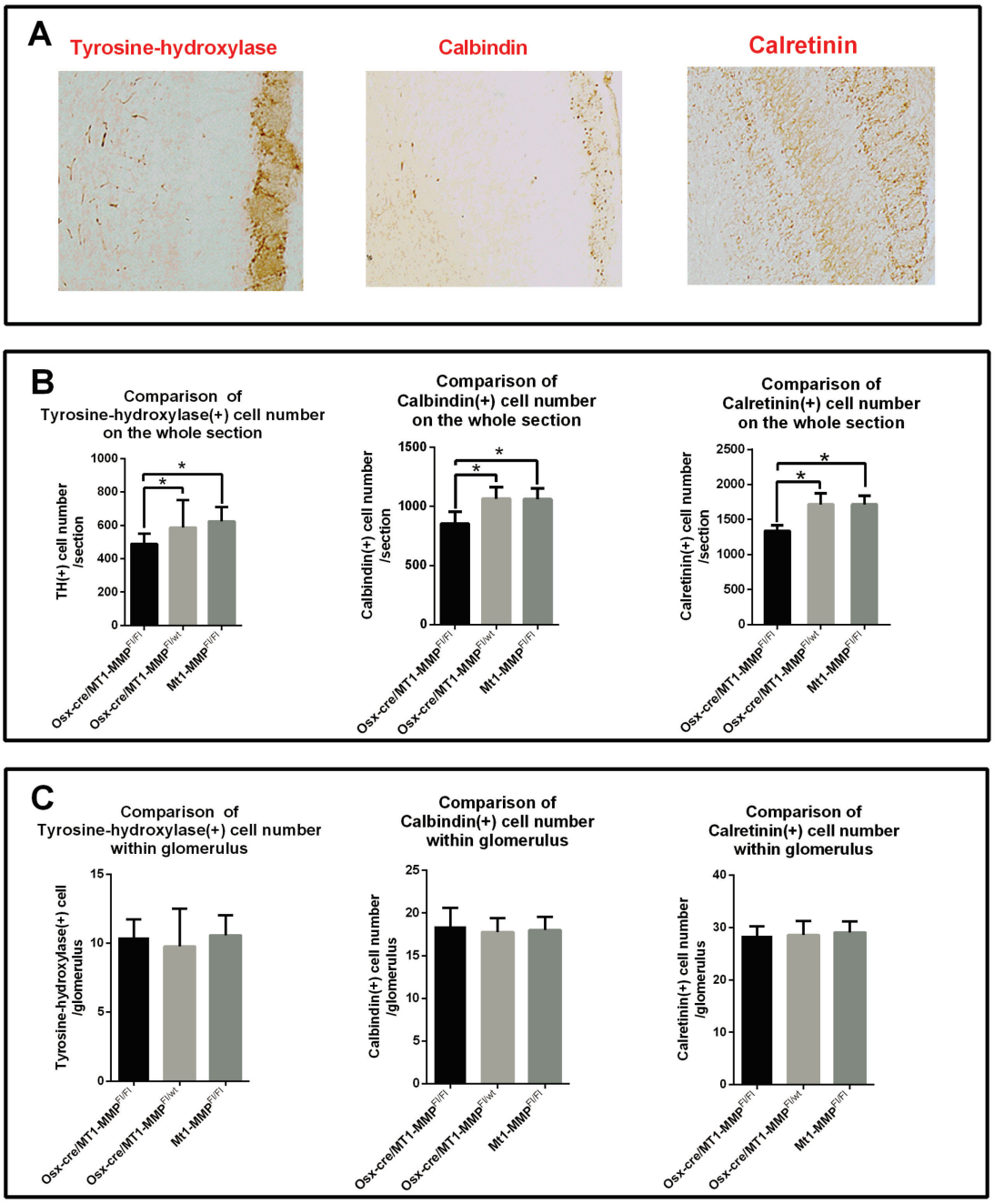

Figure 3.2.3 Comparison of Total Number and Average Number of Interneurons

Immunohistochemical staining for OB (A). The total cell number of all subtypes of interneuron was significantly reduced in the Osx-cre/MT1-MMP$^{FL/FL}$ mice compared to either the Osx-cre/MT1-MMP$^{FL/wt}$ or MT1-MMPFL/FL group; Comparison of TH (+) cell number, $p=0.0002$ and $p < 0.0001$; Comparison of calbindin (+) cell number, $p < 0.0001$; Comparison of calretinin (+) cell number $p < 0.0001$ (B). The interneuron number of all subtypes per glomeruli was not significantly changed, $p > 0.05$ (C).

3.3 SVZ Neurogenesis is Not Affected by Reduced Demand of Olfactory Interneurons.

3.3.1 BrdU Labeling NPCs

In order to investigate the proliferation rate in mouse SVZ, our previous study used germline MT1-MMP knockout mice versus relative control mice and compared the SVZ neurogenesis between them (Langenfurth et al., 2016). This study then sought to create a new conditional MT1-MMP deficient mouse model. Three groups of mice, Osx-cre/MT1-MMP$^{FL/FL}$ versus Osx-cre/MT1-MMP$^{FL/wt}$ or MT1-MMP$^{FL/FL}$ mice, were injected with BrdU. Frozen brain sections were immunochemically stained with anti BrdU antibody and signals were developed with DAB. BrdU staining revealed a broad and clear nuclear immune-reactivity in all three groups. With the aim of investigating the SVZ proliferation rate, the number of fast proliferation cells in the SVZ was then analyzed. Mice were injected i.p. with a single dose of BrdU (50 mg/kg) 2h before being euthanized. As the morphological shape of the SVZ varies in different layers, 4 stereotactic coordinates were defined for counting and comparing the BrdU positive cell numbers (see methods section). Within each coordinate, the counting point was assigned to a certain area in the anterior side of the SVZ in which BrdU positive cells were concentrated. The results showed that there was no significant different between the Osx-cre/MT1-MMP$^{FL/FL}$ group versus the Osx-cre/MT1-MMP$^{FL/wt}$ or

MT1-MMP$^{FL/FL}$ group, which indicated that the proliferation level was not affected in Osx-cre/MT1-MMP$^{FL/FL}$ mice.

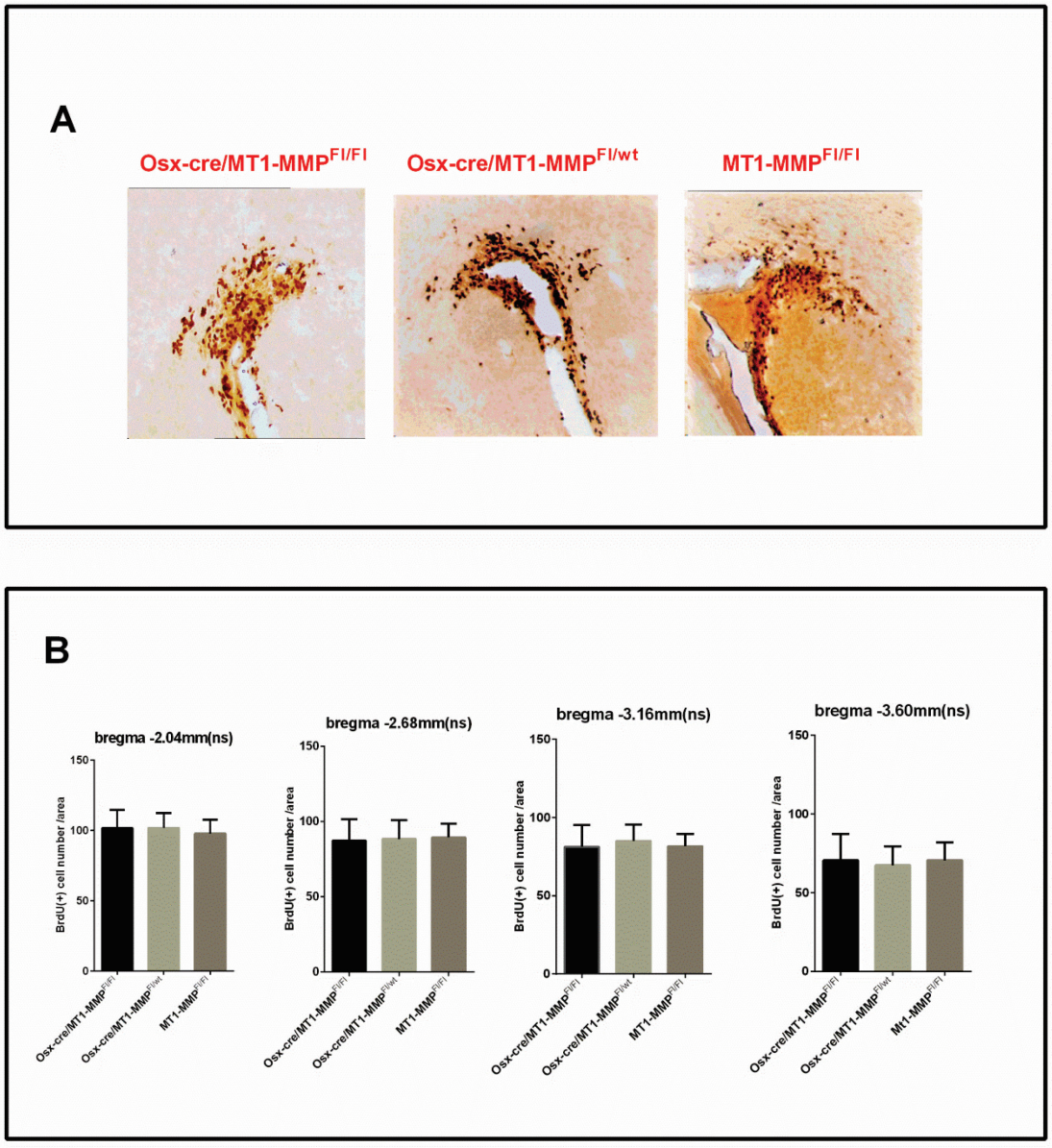

Figure 3.3.1 BrdU(+) Cell Number of Counting Point and Statistical Analysis in Selected Counting Layer

Immunohistochemical staining for BrdU. (A) The comparison of BrdU(+) cell numbers was conducted separately in each stereotactic coordinate, -2.04mm, -2.68mm, -3.16mm, -3.60mm to bregma. There was no significant different between Osx-cre/MT1-MMP$^{FL/FL}$ group and Osx-cre/MT1-MMP$^{FL/wt}$ or MT1-MMP$^{FL/FL}$ group across all 4 coordinates, $p > 0.05$ (B).

3.3.2 NPC Subtypes

This study also sought to investigate the number of NPC subtypes. For identification of type-B cells, stem cell marker nestin and Type-B cell marker GFAP were combined with BrdU staining (Lledo et al., 2006). The anti-nestin, GFAP and BrdU antibody were used and signals were developed with Alex488, Alex594 and Cy5-conjugated secondary antibodies. The number of triple positive cells was compared and it was found that there was no significant difference between the conditional MT1-MMP deficient mice and the control group. Type-C cells were marked with anti-BrdU plus neural differentiation marker Mash1 antibody (Lledo et al., 2006). FITC and Alex594 conjugated secondary antibodies were used for developing signals. Double positive cells were counted and there was no significant difference between the conditional MT1-MMP deficient mice and the control group. Similarly, type-A cells were marked with Type-A cell marker PSA-NCAM and BrdU (Lledo et al., 2006). Alex488 and Cy3-conjugated secondary antibodies were used for developing signals. Double positive cells number was then compared and there was no significant difference between the conditional MT1-MMP deficient mice and the control group. Hence, numbers of all three types of NPCs were remained unchanged in the SVZ, indicating that the SVZ neurogenesis was not altered in conditional MT1-MMP deficient mice.

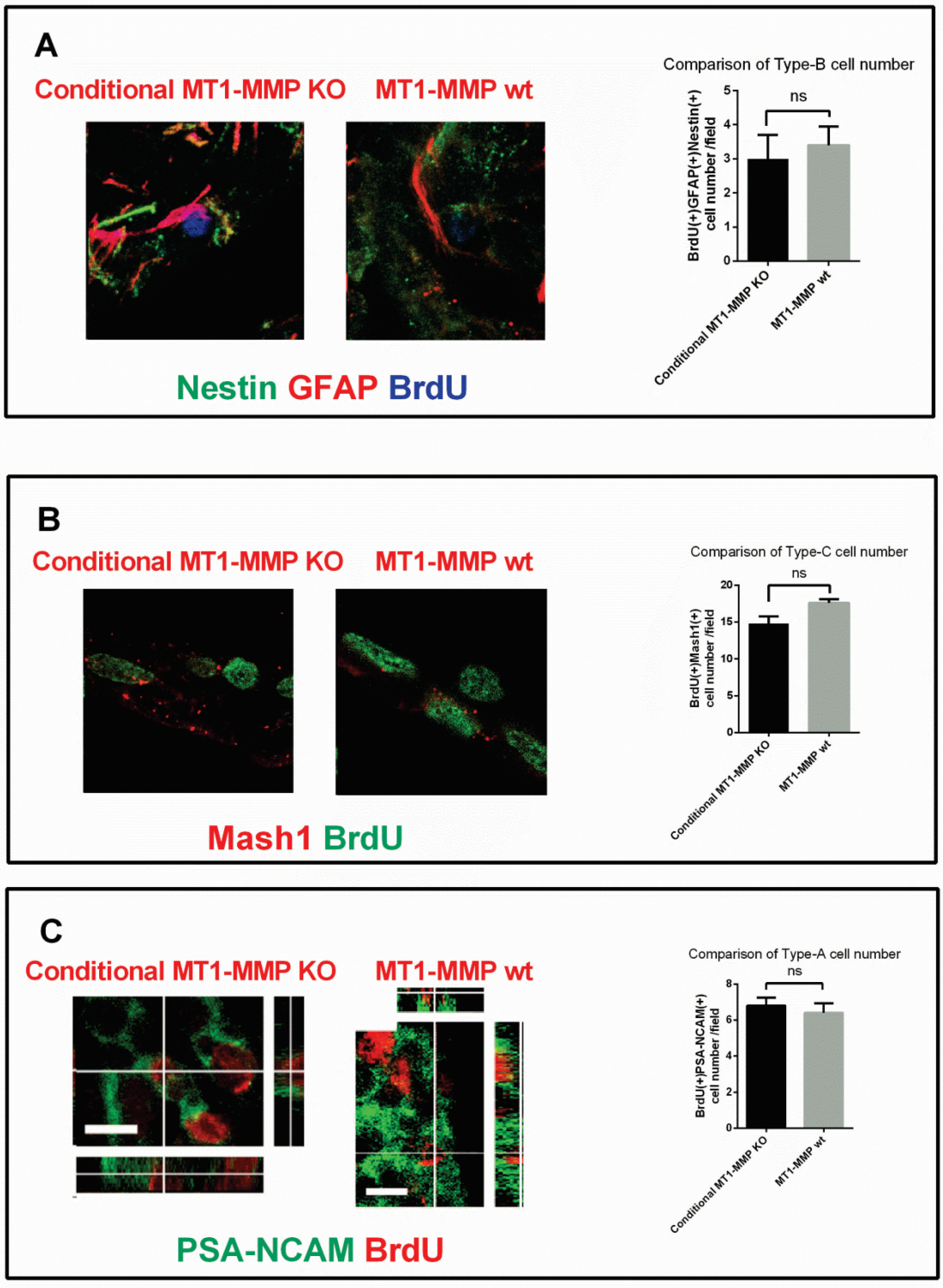

Figure 3.3.2 NPC Subtype Cell Number Comparison in SVZ

Immunoflourescent staining for type-B cells. Figures show triple positive cells. Nestin is marked in green, GFAP is marked in red and BrdU is marked in blue. The bar chart shows the statistical analysis of triple positive cell numbers. There was no significant difference in type-B cells between the conditional MT1-MMP deficient mice and the

control group, $p > 0.05$ (A). Immunoflourescent staining for type-C cells. The figures show double positive cells. BrdU is marked in green and Mash1 is marked in red. The bar chart shows the statistical analysis of double positive cell numbers. There was no significant difference of type-C cells between the conditional MT1-MMP deficient mice and the control group, $p > 0.05$ (B). Immunoflourescent staining for type-A cells. The figures show double positive cells. PSA-NCAM is marked in green and BrdU is marked in red. The bar chart shows the statistical analysis of double positive cell numbers. There was no significant difference in type-A cell between the conditional MT1-MMP deficient mice and the control group, $p > 0.05$ (C).

3.4 NPC Numbers Adapt to the Reduce Demand for New Olfactory Interneurons within the RMS

With the aim of investigating the level of migrating cells in the brain, Osx-cre/MT1-MMP$^{FL/FL}$ versus control groups were injected i.p. with 2x daily with BrdU for three days (effective dose of 50 mg/kg), with the mice then left untreated for 18 days. 21 days after the first BrdU injection the mice were euthanized and immune-labelled for BrdU detection. After this long pulsing, it is enough to label all of newly replicated DNA in NPCs migrating out from SVZ. The DNA label is chased out (each DNA replication now incorporates unlabeled nucleotides), thus migrating NPCs could then be detected after repeated application of BrdU.

3.4.1 BrdU Positive Cells in OB

In order to detect if the number of NPCs reaching the OB was affected in

conditional MT1-MMP deficient mice, quantification of BrdU positive cells in the OB was performed. More specifically, the BrdU numbers of positive cells in the Internal Plexiform Layer (IPL), External Plexiform Layer (EPL) as well as the Glomerular Layer (GL), were counted and compared separately. The results showed that there was no significant difference in NPC numbers in the IPL and EPL between Osx-cre/MT1-MMP$^{FL/FL}$ mice versus the control group. Interestingly, the NPC number was significantly reduced in the GL of Osx-cre/MT1-MMP$^{FL/FL}$ mice compared with the controls. Considering the results that the glomerulus number were significantly reduced while the cell number within the glomeruli remained constant, it can be concluded that the significant reduction of NPCs in GL was correlated by reduced number of glomeruli.

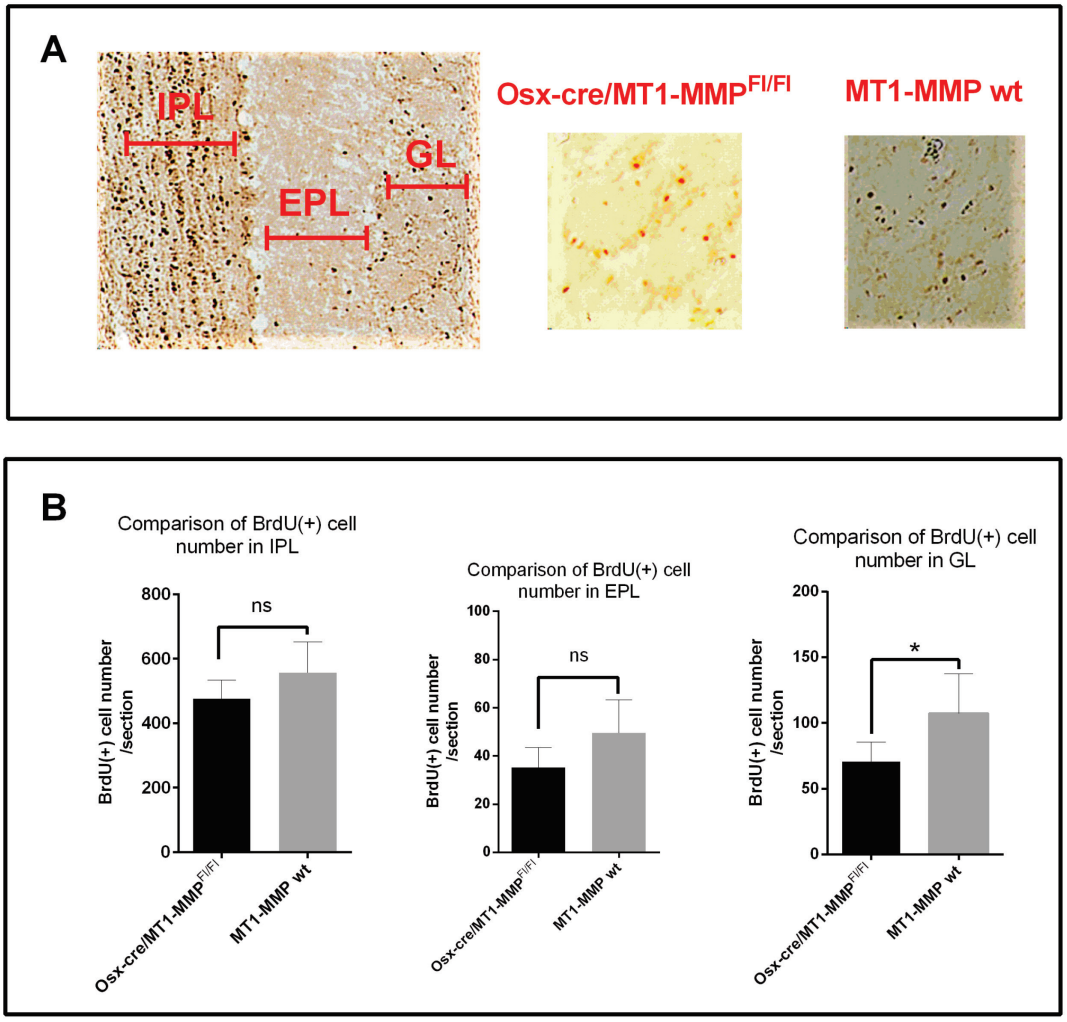

Figure 3.4.1 Detection of NPCs in OB and Statistical Analysis

Immunohistochemical staining of BrdU in OB (A). There was no significant difference in BrdU positive numbers in the IPL and EPL; The BrdU positive cell number was significantly reduced in the Osx-cre/MT1-MMP$^{FL/FL}$ mice in GL, p=0.04 (B).

3.4.2 BrdU Positive Cells in RMS

The previous results showed no difference in proliferation levels (Ki67 positive cell) in RMS and an increased cell death level (TUNEL positive cells) in RMS2 and RMS3 in MT1-MMP deficient mice compared to the controls (Langenfurth et al., 2016). To better identify migrating NPCs in

the RMS, neuronal migration marker Dcx was combined with BrdU staining. Immunofluorescent staining was then performed on Osx-cre/MT1-MMP$^{FL/FL}$ mice versus control mice. According to the location, The RMS was divided into 3 parts, RMS1 (proximal to the SVZ), RMS2 and RMS3 (distal from the SVZ). The quantification was done in 3 defined sub-regions of RMS. In RMS1 and RMS2, the numbers of double positive cells did not show any significant difference between Osx-cre/MT1-MMP$^{FL/FL}$ and the control groups. However, there was a significant reduction of double positive cell numbers in RMS3 in Osx-cre/MT1-MMP$^{FL/FL}$ mice compared to the controls. It was possible to conclude that the distal (to the SVZ) part of the RMS, especially RMS3, was the place where cell death of NPCs took place. Hence, in response to reduced demand of new interneurons, the NPC number reduced adaptively within the distal part of the RMS.

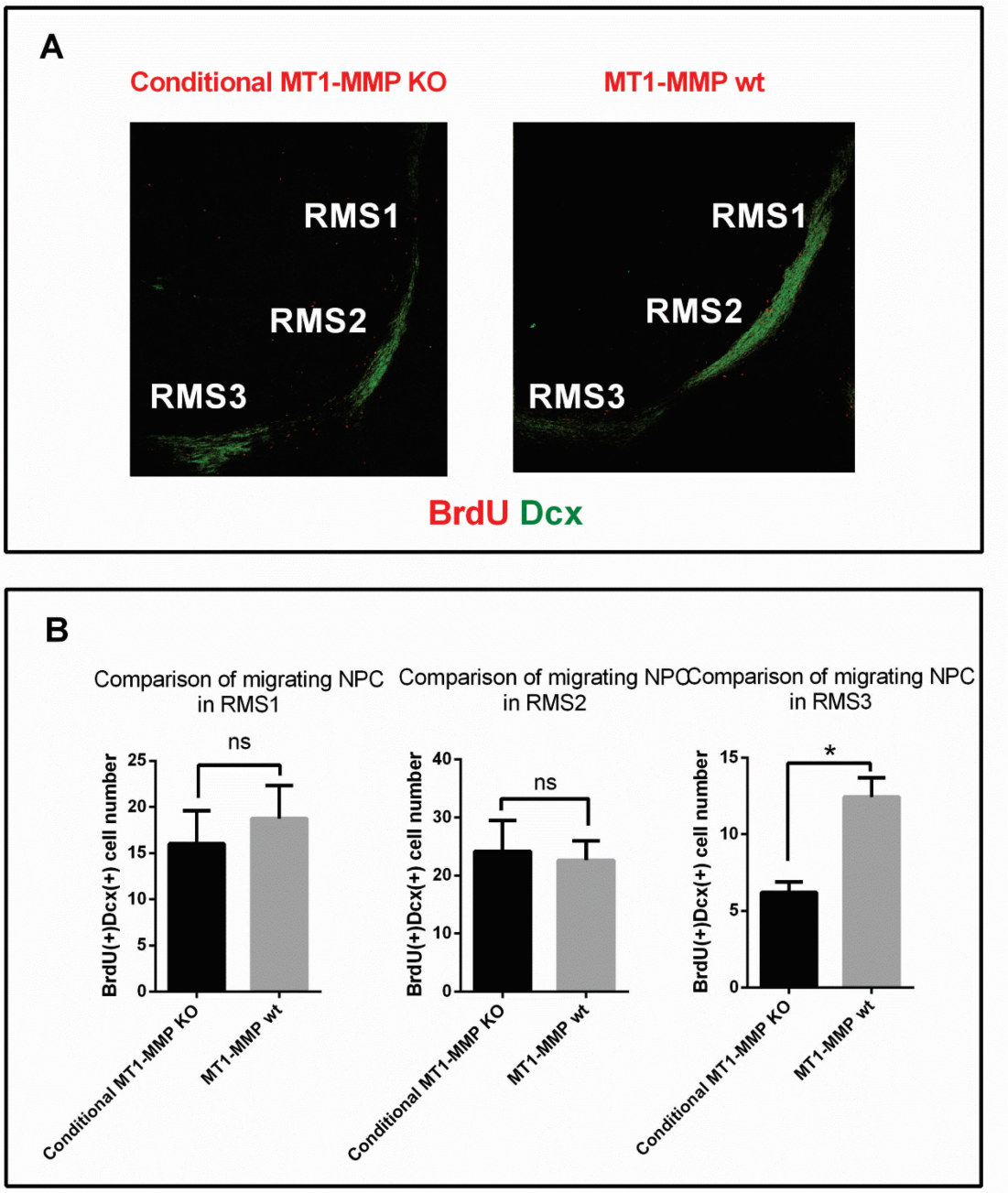

Figure 3.4.2 NPC Immunoflourescent Staining for Migrating NPCs in RMS Sub-regions and Statistical Analysis

Immunohistochemical double staining of RMS sub-regions. The Dcx was stained in green and BrdU was stained in red. (A). There was no significant difference in double positive cell numbers in RMS1 and RMS2. The double positive cell number was significantly decreased in the Osx-cre/MT1-MMP$^{FL/FL}$ mice in RMS3 (B).

3.4.3 Cell Death level in RMS

TUNEL-assays are highly reliable indicators of dying cells as they show the final stage of different cell-death programs. Our previous data showed that TUNEL(+) cells was specifically and statistically significantly increased in the distal RMS, but not in any other region of the SVZ or the RMS. (Langenfurth et al., 2016)

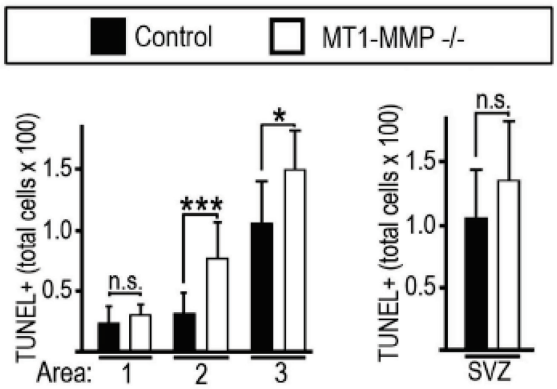

Figure 3.4.3 Cell Death Level in SVZ and RMS

There was no significant difference for TUNEL(+) cell number between MT1-MMP deficient mice and controls in SVZ. The TUNEL(+) cell number r was significantly increased in the MT1-MMP deficient mice in RMS2 ($p < 0.001$) and RMS3 ($p < 0.05$).

4. Discussion

In our study, we investigated two complementary MT1-MMP deficient mouse models, namely germline MT1-MMP knockout and conditional MT1-MMP knockout mice. To investigate the relation between the extent of periglomerular neurogenesis and NPC turnover in the SVZ and RMS, this non-invasive model was an important prerequisite. In previous studies, the role of the SVZ and RMS has been investigated through controlling periglomerular cell numbers with intracerebral injections (M. A. Hack et al., 2005), creation of cerebral lesions (Pierre-Marie, L; Merkle, F.T; Alvarez-Buylla, 2014) or through acute chemical ablation of the OE (Alonso et al., 2008). These methods can generate uncontrolled pathological stimuli which complicate the study of new RMS-derived neurons (Wlodkowic, Skommer, & Darzynkiewicz, 2012). However, with germline MT1-MMP knockout, OSNs and their innervation reduce together with the surface of the OE. Therefore, the olfactory input will be limited but does not any cause inflammation. Moreover, MMPs (including MT1-MMP) are expressed in migrating neuroblasts and facilitate in cell migration (Xu et al., 2016). The conditional MT1-MMP knockout mouse allows the ablation of MT1-MMP specifically in bone-forming osteoblasts. It can provide additional advantages for investigating NPC migration in the SVZ-RMS-OB axis as it prevents MT1-MMP deficiency in migrating NPCs. Therefore, the conditional

MT1-MMP deficient mouse can also generate a reduced number of olfactory glomeruli without causing inflammation. In addition, there is no developmental deficit in the central neural system. Thus, the conditional MT1-MMP deficient mouse is an important model that induces MT1-MMP deficiency only outside of the brain and corroborated the results obtained with the germline knockout model. In the OB of conditional MT1-MMP deficient mice, a decrease in glomeruli is consistent with reduced numbers of newly generated periglomerular cells, leading to decreased demand of NPCs from stem cell niches.

With this non-invasive model, we can describe how the central neural system responds to a decreased demand for NPCs. NPC proliferation in the SVZ and migration of NPCs towards the OB seems not to be affected by the reduced demand for NPCs, while increased cell mortality within the distal RMS was detected that could potentially affect the supply of new interneurons to the glomerular cell layer. Therefore, accelerated cell mortality in the distal RMS of MT1-MMP deficient mice can balance the number of newly generated periglomerular cells to the reduced demand for this cell-type in the OB. Through BrdU-tracking, we found that reduced numbers of new-born cells correlate with the altered glomeruli numbers in MT1-MMP deficient mice, while no differences were detected in all other layers of the OB across all models. In the case that

reduced numbers of new neurons arrive at their periglomerular destination, this situation can be caused by decreased neurogenesis, slowed migration or increased cell death. By three different BrdU-labelling protocols we found no indication for altered proliferation-rates in the SVZ, RMS and OB, which is also confirmed by the quantification of the proliferation marker Ki67. Also, total cell-numbers in these regions were unchanged. Next, we investigated the RMS morphology and potential differences in migration of NPCs. The RMS is maintained by astrocytes forming tube-like structures which guide the neuroblasts to their final destination in the OB. Arrested migration of NPCs together with a continuous recruitment of newborn NPCs in the SVZ should be visible as an enlargement in the size of the RMS (Kirschenbaum, Doetsch, Lois, & Alvarez-Buylla, 1999). However, the morphology of the RMS proximal to the SVZ and the intermediate part of the RMS remained similar in all models (BrdU-tracking of DCX-labeled cells in the distal RMS even revealed a reduction of neuroblast cell numbers in MT1-MMP deficient animals). Also, a combined alteration in proliferative and migratory behavior of NPCs can be excluded, as this would have been detected by altered cell-division levels in the short or long-term BrdU labeling, or Ki67 immunohistochemistry. After ruling out that any statistically significant effects in proliferation or migration of NPCs in the SVZ or large parts of

the RMS was taking place, we studied cell mortality in the olfactory neurogenic axis. TUNEL-assays are highly reliable indicators of dying cells as they show the final stages of different cell mortality programs. We found that the number of TUNEL(+) cells saw a specific and statistically significant increase in the distal RMS, but not in any other region of the SVZ or the RMS. Thus, our study suggests a signaling mechanism between the glomerular layer of the OB and the distal RMS irrespective of SVZ neurogenesis, which can relay information on a reduced demand for periglomerular neurons to the germinative center in the RMS.

One possible mechanism is the release of chemoattractants in the OB. One important chemoattractant leading sub-ventricular NPCs into the RMS is sonic hedgehog and it has been proven that PSA-NCAM positive migrating neuroblasts express the receptor of sonic hedgehog (Angot et al., 2008). Since our results already show that the NPC number in proximal RMS (RMS1) is unchanged in conditional MT1-MMP deficient mice, this indicates that the number of NPCs migrating into the RMS remains unchanged, and the expression level of sonic hedgehogs in the SVZ should not change as well. During the migration progress, NPCs are directed towards the OB with the guidance of prokineticin-2, Netrin1, and GDNF, which are produced by the OB (Murase & Horwitz, 2002; K. L.

Ng et al., 2005; Paratcha et al., 2006). A decreased final total number of NPCs reaching the OB in MT1-MMP deficient mice as compared with the controls was detected, and we showed that this reduction in NPCs is due to increased cell mortality in the RMS. On this basis it is reasonable to hypothesize that the OB-derived chemoattractants may be involved in the survival and differentiation of NPCs. GDNF has already been shown to promote the survival and differentiation of dopaminergic neurons in culture, thus further studies may focus on this protein (Paratcha et al., 2006). After reaching the OB, type-A cells radially migrate out from the RMS toward the granule cell layer under the control of several extra-cellular matrix (ECM) proteins such as Reelin, Tenascin-R, and Prokineticin-2 from the RMS (I. Hack et al., 2002; Lledo et al., 2006; K. L. Ng et al., 2005). Although the NPC number is only reduced in the GL but not in all other layers of the OB, the total number of NPCs detached from the RMS likely is also reduced. The expression level of these ECMs thus needs to be further investigated. The size of the OB is significantly affected in our mouse model as compared with controls, while the RMS size seems to be unaffected. Thus the reduced demand for olfactory interneurons is most probably related to the role of chemoattractants, especially diffusible proteins produced by the OB (Murase & Horwitz, 2002; K. L. Ng et al., 2005).

Moreover, recently a new mechanism driving neural network activity, namely respiration-entrained rhythm (RR), has been discovered which is distinct from the theta oscillations in the brain. RR is largely related to neurons in the OE, OB, and cortex, and driven by respiration it can be recorded in the OB, prelimbic cortex (PLC), parietal cortex (PAC), and dorsal hippocampus (Zhong et al., 2017). Thus RR is thought to be related not only to respiration and olfaction but also some cognitive–behavioral functions. In previous studies, respiration was limited and animals breathed only with their mouths. The results showed a direct correlation between RR and respiration. However, this model is not ideal for further investigation of cognitive–behavioural studies as rodents detect a lot of information through smell perception rather than visual information. In addition, respiration deprivation can have a negative influence on animals when they are taking behavioral tests, such as certain puzzles. Respiration deprivation is also not helpful for performing long-term analysis, such as intelligence development tests. Thus, our model provides a natural respiration status with a reduced number of neurons which can better investigate the relation between RR and respiration, cognitive–behavioral functions and even intelligence development.

5. Summary

In this study, I explored the level of SVZ neurogenesis, NPC migration and the number of olfactory interneurons in a model with modulated olfactory inputs, namely the conditional MT1-MMP mouse model. Our results showed that the size of the OB was significantly reduced, as well as the glomerulus number within the OB in MT1-MMP deficient mice as compared to controls. Also, the total number of interneurons and migrating NPCs was significantly reduced within the OB of MT1-MMP knockout mice, which closely related to a reduced number of glomeruli. Our results support the conclusion that the reduced number of interneurons in the OB after MT1-MMP ablation is not caused by any developmental deficits in the olfactory sensory system or any inflammation, but rather by reduced olfactory input. Furthermore, this reduction of interneuron cell numbers generates a reduced demand for new neurons differentiating from migrating NPCs.

Similarly, our results showed that there was no significant difference in NPCs proliferation and migration between the Osx-cre/MT1-MMP$^{FL/FL}$ group versus the Osx-cre/MT1-MMP$^{FL/wt}$ or MT1-MMP$^{FL/FL}$ group. This indicated that the proliferation level is not affected in conditional MT1-MMP deficient mice in response to reduced demand for new neurons. In particular, all three types of NPCs were unaltered in the SVZ,

indicating that SVZ neurogenesis was not altered in conditional MT1-MMP deficient mice.

Finally, in the OB, there was no significant difference of NPC numbers in the IPL and EPL but the number of NPCs saw significant reduction only in the GL of Osx-cre/MT1-MMP$^{FL/FL}$ mice. This significant reduction of migrating NPCs in the GL was closely related to reduced glomeruli numbers. The reduced number of migrating NPCs also indicates reduced demand for new interneurons. In response to this reduced demand, NPC numbers reduced adaptively within the distal part of the RMS.

Altogether, we can conclude that there is an adaptive response for the reduced demand of periglomerular neurons in the RMS while NPC proliferation and migration in the SVZ is not affected.

6. Reference

Alonso, M., Ortega-Perez, I., Grubb, M. S., Bourgeois, J.-P., Charneau, P., & Lledo, P.-M. (2008). Turning Astrocytes from the Rostral Migratory Stream into Neurons: A Role for the Olfactory Sensory Organ. *Journal of Neuroscience*, *28*(43), 11089–11102. https://doi.org/10.1523/JNEUROSCI.3713-08.2008

Alvarez-Buylla, A., & Lim, D. A. (2004). For the long run: Maintaining germinal niches in the adult brain. *Neuron*, *41*(5), 683–686. https://doi.org/10.1016/S0896-6273(04)00111-4

Angot, E., Loulier, K., Nguyen-Ba-Charvet, K. T., Gadeau, A.-P., Ruat, M., & Traiffort, E. (2008). Chemoattractive Activity of Sonic Hedgehog in the Adult Subventricular Zone Modulates the Number of Neural Precursors Reaching the Olfactory Bulb. *Stem Cells*, *26*(9), 2311–2320. https://doi.org/10.1634/stemcells.2008-0297

Arvidsson, A., Collin, T., Kirik, D., Kokaia, Z., & Lindvall, O. (2002). Neuronal replacement from endogenous precursors in the adult brain after stroke. *Nature Medicine*, *8*(9), 963–970. https://doi.org/10.1038/nm747

Belvindrah, R., Lazarini, F., & Lledo, P.-M. (2009). Postnatal neurogenesis: from neuroblast migration to neuronal integration. *Reviews in the Neurosciences*, *20*(5–6), 331–346. https://doi.org/10.1515/REVNEURO.2009.20.5-6.331

Crane, P. K., Gibbons, L. E., Dams-O'Connor, K., Trittschuh, E., Leverenz, J. B., Keene, C. D., … Larson, E. B. (2016). Association of Traumatic Brain Injury With Late-Life Neurodegenerative Conditions and Neuropathologic Findings. *JAMA Neurology*, *73*(9), 1062. https://doi.org/10.1001/jamaneurol.2016.1948

DeMaria, S., & Ngai, J. (2010). The cell biology of smell. *Journal of Cell Biology*, *191*(3), 443–452. https://doi.org/10.1083/jcb.201008163

Doetsch, F., García-Verdugo, J. M., & Alvarez-Buylla, a. (1997). Cellular composition and three-dimensional organization of the subventricular germinal zone in the adult mammalian brain. *The Journal of Neuroscience : The Official Journal of the Society for Neuroscience*, *17*(13), 5046–5061.

Galvan, V., & Jin, K. (2007). Neurogenesis in the aging brain. *Clinical Interventions in Aging*. https://doi.org/10.2147/CIA.S1614

Gkantidis, N., Blumer, S., Katsaros, C., Graf, D., & Chiquet, M. (2012). Site-Specific Expression of Gelatinolytic Activity during Morphogenesis of the Secondary Palate in the Mouse Embryo. *PLoS ONE*, *7*(10). https://doi.org/10.1371/journal.pone.0047762

Glass, R., & Synowitz, M. (2014). CNS macrophages and peripheral myeloid cells in brain tumours. *Acta Neuropathologica*. https://doi.org/10.1007/s00401-014-1274-2

Gon??alves, J. T., Schafer, S. T., & Gage, F. H. (2016). Adult

Neurogenesis in the Hippocampus: From Stem Cells to Behavior. *Cell*. https://doi.org/10.1016/j.cell.2016.10.021

Graeber, M. B., & Streit, W. J. (2010). Microglia: Biology and pathology. *Acta Neuropathologica*. https://doi.org/10.1007/s00401-009-0622-0

Hack, I., Bancila, M., Loulier, K., Carroll, P., & Cremer, H. (2002). Reelin is a detachment signal in tangential chain-migration during postnatal neurogenesis. *Nature Neuroscience*, *5*(10), 939–945. https://doi.org/10.1038/nn923

Hack, M. A., Saghatelyan, A., de Chevigny, A., Pfeifer, A., Ashery-Padan, R., Lledo, P.-M., & Götz, M. (2005). Neuronal fate determinants of adult olfactory bulb neurogenesis. *Nature Neuroscience*, *8*(7), 865–872. https://doi.org/10.1038/nn1479

Holmbeck, K., Bianco, P., Caterina, J., Yamada, S., Kromer, M., Kuznetsov, S. A., … Birkedal-Hansen, H. (1999). MT1-MMP-deficient mice develop dwarfism, osteopenia, arthritis, and connective tissue disease due to inadequate collagen turnover. *Cell*, *99*(1), 81–92. https://doi.org/10.1016/S0092-8674(00)80064-1

Kazanis, I. (2009). The subependymal zone neurogenic niche: A beating heart in the centre of the brain. *Brain*, *132*(11), 2909–2921. https://doi.org/10.1093/brain/awp237

Kirschenbaum, B., Doetsch, F., Lois, C., & Alvarez-Buylla, A. (1999). Adult subventricular zone neuronal precursors continue to proliferate

and migrate in the absence of the olfactory bulb. *The Journal of Neuroscience : The Official Journal of the Society for Neuroscience*, *19*(6), 2171–80. Retrieved from http://www.ncbi.nlm.nih.gov/pubmed/10066270

Klempin, F., & Kempermann, G. (2007). Adult hippocampal neurogenesis and aging. *European Archives of Psychiatry and Clinical Neuroscience*. https://doi.org/10.1007/s00406-007-0731-5

Kriegstein, A., & Alvarez-buylla, A. (2011). The Glial Nature of Embryonic and Adult Neural Stem Cells. *Annual Reviews of Neuroscience*, 149–184. https://doi.org/10.1146/annurev.neuro.051508.135600.The

Langenfurth, A., Gu, S., Bautze, V., Zhang, C., Neumann, J. E., Schüller, U., … Glass, R. (2016). Decreased demand for olfactory periglomerular cells impacts on neural precursor cell viability in the rostral migratory stream. *Scientific Reports*, *6*(1), 32203. https://doi.org/10.1038/srep32203

Lazarini, F., & Lledo, P. M. (2011). Is adult neurogenesis essential for olfaction? *Trends in Neurosciences*. https://doi.org/10.1016/j.tins.2010.09.006

Lledo, P.-M., Alonso, M., & Grubb, M. S. (2006). Adult neurogenesis and functional plasticity in neuronal circuits. *Nature Reviews Neuroscience*, *7*(3), 179–193. https://doi.org/10.1038/nrn1867

Luxenhofer, G., Breer, H., & Strotmann, J. (2008). Differential reaction of outgrowing olfactory neurites monitored in explant culture. *Journal of Comparative Neurology*, *509*(6), 580–593. https://doi.org/10.1002/cne.21766

Murase, S., & Horwitz, A. F. (2002). Deleted in colorectal carcinoma and differentially expressed integrins mediate the directional migration of neural precursors in the rostral migratory stream. *The Journal of Neuroscience : The Official Journal of the Society for Neuroscience*, *22*(9), 3568–3579. https://doi.org/20026349

Ng, C., Sandoval, K., Rowitch, D. H., Xu, D., Patrick, S., Huang, E. J., & Alvarez-buylla, A. (2017). frontal lobe, *354*(6308), 1–14. https://doi.org/10.1126/science.aaf7073.Extensive

Ng, K. L., Li, J.-D., Cheng, M. Y., Leslie, F. M., Lee, A. G., & Zhou, Q.-Y. (2005). Dependence of olfactory bulb neurogenesis on prokineticin 2 signaling. *Science (New York, N.Y.)*, *308*(5730), 1923–7. https://doi.org/10.1126/science.1112103

Oboti, L., Peretto, P., de Marchis, S., & Fasolo, A. (2011). From chemical neuroanatomy to an understanding of the olfactory system. *European Journal of Histochemistry*, *55*(4), 194–199. https://doi.org/10.4081/ejh.2011.e35

Paratcha, G., Ibáñez, C. F., & Ledda, F. (2006). GDNF is a chemoattractant factor for neuronal precursor cells in the rostral

migratory stream. *Molecular and Cellular Neuroscience*, *31*(3), 505–514. https://doi.org/10.1016/j.mcn.2005.11.007

Pierre-Marie, L; Merkle, F.T; Alvarez-Buylla, A. (2014). NIH Public Access. *Trends Neuroscience*, *31*(8), 392–400. https://doi.org/10.1016/j.tins.2008.05.006.Origin

Ramírez-Castillejo, C., Sánchez-Sánchez, F., Andreu-Agulló, C., Ferrón, S. R., Aroca-Aguilar, J. D., Sánchez, P., … Fariñas, I. (2006). Pigment epithelium-derived factor is a niche signal for neural stem cell renewal. *Nature Neuroscience*, *9*(3), 331–9. https://doi.org/10.1038/nn1657

Sanai, N., Nguyen, T., Ihrie, R. a, Mirzadeh, Z., Tsai, H., Wong, M., … Alvarez-buylla, A. (2012). NIH Public Access. *Letter*, *478*(7369), 382–386. https://doi.org/10.1038/nature10487.Corridors

Wang, T. W., Zhang, H., Gyetko, M. R., & Parent, J. M. (2011). Hepatocyte growth factor acts as a mitogen and chemoattractant for postnatal subventricular zone-olfactory bulb neurogenesis. *Molecular and Cellular Neuroscience*, *48*(1), 38–50. https://doi.org/10.1016/j.mcn.2011.06.003

Weller, M., Wick, W., Aldape, K., Brada, M., Berger, M., Pfister, S. M., … Reifenberger, G. (2015). Glioma. *Nature Reviews Disease Primers*, 15017. https://doi.org/10.1038/nrdp.2015.17

Wlodkowic, D., Skommer, J., & Darzynkiewicz, Z. (2012). Cytometry of

apoptosis. Historical perspective and new advances. *Experimental Oncology*. https://doi.org/10.1016/j.biotechadv.2011.08.021.Secreted

Wojtowicz, J. M., & Kee, N. (2006). BrdU assay for neurogenesis in rodents. *Nature Protocols*, *1*(3), 1399–405. https://doi.org/10.1038/nprot.2006.224

Xu, H., Snider, T. N., Wimer, H. F., Yamada, S. S., Yang, T., Holmbeck, K., & Foster, B. L. (2016). Multiple essential MT1-MMP functions in tooth root formation, dentinogenesis, and tooth eruption. *Matrix Biology*, *52–54*, 266–283. https://doi.org/10.1016/j.matbio.2016.01.002

Zhang, R. L., Zhang, Z. G., Wang, Y., LeTourneau, Y., Liu, X. S., Zhang, X., … Chopp, M. (2007). Stroke Induces Ependymal Cell Transformation into Radial Glia in the Subventricular Zone of the Adult Rodent Brain. *Journal of Cerebral Blood Flow & Metabolism*, *27*(6), 1201–1212. https://doi.org/10.1038/sj.jcbfm.9600430

Zhong, W., Ciatipis, M., Wolfenstetter, T., Jessberger, J., Müller, C., Ponsel, S., … Draguhn, A. (2017). Selective entrainment of gamma subbands by different slow network oscillations. *Proceedings of the National Academy of Sciences of the United States of America*. https://doi.org/10.1073/pnas.1617249114

7. Acknowledgement

Herein I would like to express my sincere and humble acknowledgements to all those who helped me during my stay in Munich. Without their helps, I could not have believed that I can go on well with my project and finish my doctoral thesis.

My deepest gratitude goes first and foremost to Professor Rainer Glaß, my supervisor, for his constant encouragement and guidance. Without her consistent and illuminating instruction, this thesis could not have reached its present form. Also, he offered me a lot of help when I first arrived at Munich and meet the real tough time in my life.

Second, I would like to appreciate to Dr. Ulrich Schüller for his contribution and cooperation in this program. Also, I learned a lot from him in the seminar in which our lab and his group can do scientific disscusions.

Then, I would like to express my heartfelt gratitude to Dr. Roland Kälin and other colleagues in our lab. Dr. Kaelin and Lange Stefanie tought me many experimental methods and techniques. Yuping Li, Mengzhuo Hou, Yingxi Wu, Katharina Eisenhut, Marie Volmar, Ramazan Uyar, Giorgia Mastrella, Min Li, and Linzhi Cai all help me a lot in the past three years. They bring me a wonderful time in my life and I will keep in my heart forever.

Last my thanks would go to my beloved family for their loving considerations and great confidence in me all through these years. I would like to express my thanks to my beloved family for their continued support and concern for so many years. And I am grateful to everyone who helped me during my difficult time.

8. Curriculum Vitae

Name: Song Gu

Education

1.2013/9-Now ， Ludwig-Maximilians-Universität München ， Neuroscience, Supervisor：Prof. Rainer Glass

2.2012/9 – 2013/9 ， Ruprecht-Karls-Universität Heidelberg ， Translational Medicine Research， Supervisor：Prof. Jonathan Sleeman

3.2005/9 – 2012/7， Anhui Medical University， Clinical Medicine， Supervisor：Prof. Chaoshi Niu

Awards and Certificate

2014--2017: Scholarship of CSC (China Scholarship Council).

2016: the Qualification Certificate and the License Certificate

Research skills

1. Good command of basic experimental methods and skills such as Animal experiments, Tumor Inoculation, Immunochemistry, Immunoflourescent, and cell culture.

2. Master basic motheds of medicine statistics and epidemiology.

Publications

(1) The Pathology, Imaging and Treatment of Pilocytic astrocytoma and its subtype，Chinese Journal of Stereotactic and Functional Neurosurgery，2012，25（1）：52-55

(2) Decreased demand for olfactory periglomerular cells impacts on neural precursor cell viability in the rostral migratory stream. Sci Rep. 2016 Aug 30; 6:32203.

(3)Monitoring of Tumor Growth with [18F]-FET PET in a Mouse Model of Glioblastoma: SUV Measurements and Volumetric Approaches. Front. Neurosci., 14 June 2016